Comparative study of single Cu, Ag, Au, and K atoms adsorbed on Si(111)-(7×7)

G. Chen,[1,3] Xudong Xiao,[2] Y. Kawazoe,[1] X. G. Gong,[4] and C. T. Chan[3]
[1]*Institute for Materials Research, Tohoku University, Aoba-ku, Sendai 980-8577, Japan*
[2]*Department of Physics, The Chinese University of Hong Kong, Shatin, Hong Kong, China*
[3]*Department of Physics, William Mong Institute of Nano Science and Technology, Hong Kong University of Science and Technology, Hong Kong, China*
[4]*Department of Physics, Surface Physics Laboratory, Fudan University, 200433-Shanghai, China*
(Received 23 September 2008; revised manuscript received 22 January 2009; published 3 March 2009)

Using first-principles calculations, we have studied the geometrical, electronic, and dynamic properties in detail for a single K, Cu, Ag, and Au atoms adsorbed on Si(111)-7×7 surface. We have found that single noble metal Cu, Ag, and Au atoms favor the multicoordinate adsorption sites to saturate the maximum number of dangling bonds on Si(111)-(7×7) surface. For Cu, Ag, and Au atoms adsorbed on the stable or metastable adsorption sites, the bright spots in the simulated negative bias scanning tunnel microscopy (STM) images are found right on the nearby Si adatoms which are induced by a combination of the charge redistribution and the height increase in Si adatoms induced by the single metal-atom adsorption. The finite increase in charge density between Cu, Ag, and Au atoms and the nearby bonding Si atoms indicate the bond is covalent in nature. In comparison, an alkali metal K atom loses its *s* electron to the Si surface, and the charge transfer results in the bright spot at the Si adatom in simulated negative bias STM image.

DOI: 10.1103/PhysRevB.79.115301 PACS number(s): 68.43.Bc, 68.37.Ef, 73.20.At, 68.43.Fg

I. INTRODUCTION

Recently, self-organized nanoclusters on surfaces have aroused great interests for their potential applications in micro- or nanoelectronics, ultrahigh-density memories, and nanocatalysts.[1–6] In particular, the Si(111)-(7×7) surface is believed to be one of the best templates for growing diverse self-assembly structures for the next generation devices due to its large periodic unit cell and the distinct bonding sites.[4–6] However, the growth mechanisms of these self-assembly nanoclusters remain elusive.[7–11] The key step to understand the microscopic nature of these structures is to study the interaction between the adsorbate atom and the supporting surface, which actually controls the dynamical behavior of the initial stage of growth. As a powerful tool in surface science, scanning tunneling microscopy (STM) is often used to image the adsorption of metallic atoms. While a naive interpretation of the STM experimental result could often work well by assuming that the bright spots in STM image correspond to surface atoms,[12] the STM image can nevertheless be influenced by the electronic structure as well as the geometrical structure. STM measures the local density of states near the *Fermi* level rather than the atom itself.[13] By introducing foreign atoms on a surface, the electronic structure of the surface can be altered. The mismatching of real adsorbate atom with the bright spot of STM image was found in many systems.[8,9,14–17] The interpretation of STM images usually requires theoretical simulations, especially the first-principles simulations.[13]

The Si(111)-(7×7) reconstruction is well described by the dimer-adatom stacking-fault (DAS) model[18] which consists of two alternative triangular basins, namely, unfaulted half unit cell (UHUC) and faulted half unit cell (FHUC). The latter has a stacking fault between the third and fourth Si layers from the surface. There is a dimer row along the edge between the two half unit cells and a corner hole in the adjacent basin between UHUC and FHUC. This reconstruction reduces the number of dangling bonds from 49 to 19. When an extra atom is absorbed, one may intuitionally suggest that the adsorbate should sit on top the dangling bond, especially for a valence-one element adsorbate atom. However, Cho and Kaxiras[15,16] reported a different picture based on their first-principles calculations of Si(111) surface using a (4×4) unit cell rather than the full (7×7) unit cell. They found that K, Mg, Ga, Si, and Ge would like to sit on multicoordinate sites, T_4 type for K, Ga, H_3 type for Mg, and B_2 type for Si and Ge. The adsorption atop dangling bond is energetically unfavorable. In the case of hydrogen, many studies[19–25] have shown that H atom is adsorbed on top of the dangling bond. There is only one single valence electron for the H atom, and it can saturate the dangling bond by forming a covalent bond. By placing the H atom on top the corner Si adatom, the simulated charge density indeed showed that most charge is accumulated between H and Si atoms.[14] Considering the small size and electronegativity[26] of hydrogen, which is 2.20 and comparable to that of silicon (1.90), the covalent bonding nature of H-Si is reasonable. For the alkali-metal atoms, the situation is different. K was found to sit at T_4-type site.[15,16] Experimentally, Wu *et al.*[17] found that atop dangling-bond site is unfavorable for Na atom. The electronegativities[26] of Na and K are 0.93 and 0.82, respectively, which is very small compared to that of Si. This means that the charge of alkali-metal atoms could be transferred to the Si surface and the bond formed between the cation of alkali-metal atom and the surface is ionic in nature, leading to a multicoordinate site adsorption.

Silver and gold are two frequently used metallic elements to form electrodes on semiconductor surface.[12] The detailed atomic-scale knowledge of adsorption of single Cu, Ag, and Au atoms on highly reconstructed semiconductor Si(111)-(7×7) surface is important not only for the sake of a theoretical understanding but also device level technological application. With the electronegativities[26] of Cu, Ag, and

Au being 1.90, 1.93, and 2.40, which are comparable to the value of 2.20 of H and 1.90 of Si, it is hard to judge whether there will be any charge transfer to Si surface from these atoms with a closed inner electronic shell but one outermost *s* electron. We reported in an early letter[14] that experimental STM images showed bright spots at the atop Si adatom sites under negative bias, which seems to support that the monovalence Cu, Ag, and Au atoms sit on top of the dangling bonds of the Si adatoms. Using first-principles calculations, however, we found that these single atoms actually were adsorbed on the multicoordinate sites saturating a maximum number of dangling bonds around them. The adsorption of metal atom pushes the nearby Si adatom outward and induces a redistribution of charge density locally. By placing the metal atom on its stable and the metastable multicoordinate adsorption sites, we simulated the STM images and found bright spot upon the Si adatom under negative bias. The simulated images under positive bias, however, show bright spot at the adsorbed atom positions, also in agreement with experimental observations. In this paper, we report our detailed theoretical investigation of Cu, Ag, and Au atoms adsorbed on Si(111)-(7×7) surface. The results of K atom are also included for comparison.

II. DETAILS OF CALCULATIONS

Our spin-polarized first-principles calculations are performed based on the density-functional theory (DFT),[27,28] which is implemented in the Vienna *ab initio* simulation package (VASP).[29,30] We have employed the projector augmented-wave (PAW) method.[31,32] The exchange correlation is calculated using the generalized gradient approximation with the Perdew, Burke, and Ernzerhof parameterization (PBE-GGA).[33] The solution of the Khon-Sham equations is calculated by an efficient matrix diagonalization technique based on a sequential band-by-band residual minimization method.[30] A repeated slab geometry is used, with six Si layers separated by a 12 Å vacuum, which is large enough to eliminate the interaction of adsorbed atoms with the periodic images of surface. The unit cell consists of 298 Si atoms in the DAS model and 49 H atoms that terminate the bottom Si layer. The wave functions are expanded in a plane-wave basis with an energy cutoff of 250.0 eV for K, Ag, and Au, and 273 eV for Cu. Only the Γ point is used in the summation of the Brillouin zone of the simulation cell. The silicon atoms in bottom layer of the unit cell are fixed to model the bulk lattice property, while all the other atoms are fully relaxed. The optimization is stopped when the forces acting on each atom fall below 0.02 eV/Å.

In order to test the accuracy of the method, we have first calculated the lattice constants, which are 5.31 Å for K bcc structure, 5.47 Å for Si diamond structure, and 3.64, 4.16, and 4.17 Å, respectively, for Cu, Ag, and Au fcc structures. These agree well with the experimental structural parameters (5.23, 5.43, 3.61, 4.09, and 4.08 Å for K, Si, Cu, Ag, and Au, respectively).[26] The molecular bond lengths for SiH, SiCu, SiAg, and SiAu molecules are calculated to be 1.55, 2.18, 2.36, and 2.25 Å, which are also in good agreement with the experimental data 1.52, 2.28, 2.40, and 2.26 Å, respectively.[26,34,35] The SiK has a bond length around 3.05 Å being close to the previously reported theoretical length of 3.13 Å.[36]

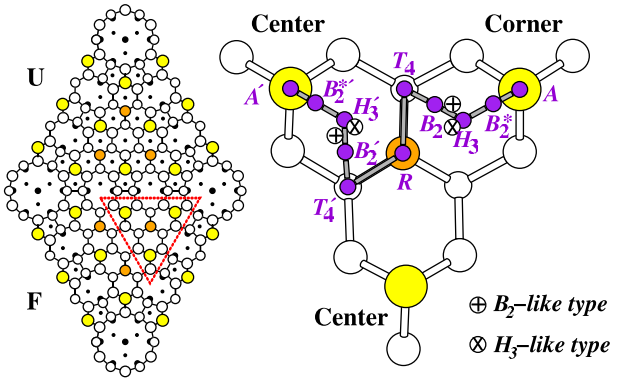

FIG. 1. (Color online) The schematic atomic configuration of DAS unit cell, and the studied adsorption sites. For clarity, only the upper four Si layers plus the Si adatoms are shown. The area defined by the triangle is enlarged on the right side, which is representative to illustrate the adsorption sites. The on-top Si adatom sites, on-top Si rest atom sites, bridge sites, hollow sites, and threefold sites are labeled by A-, R-, B_2-, H_3-, and T_4-type sites, respectively. The preferable adsorption sites are H_3-like or B_2-like sites for Cu, Ag, and Au atoms are schematically marked.

III. RESULTS AND DISCUSSIONS

A. Adsorption sites

Figure 1 shows the schematic atomic structure of the DAS model. For clarity, only the upper four layers of Si(111)-(7×7) plus the Si adatoms are presented. The basin defined by the triangle is enlarged at the right side of Fig. 1, on which we labeled the studied adsorption sites in this paper. By symmetry, basins outside the triangle can find their equivalent sites inside the triangle. Except for the on-top Si adatom site (A type) and the on-top Si rest atom (R type), we shall follow the definition of Cho and Kaxiras[15,16] referring the bridge site as B_2 type, the hollow site as H_3 type (the center of Si hexagonal ring on surface), and the threefold site around Si rest atom as T_4 type. By fully relaxing the structures, we found that for Cu, Ag, and Au single metal atoms, the best adsorption sites are either B_2-like sites which lie between the H_3-type site and its nearby B_2-type site or the H_3-like sites which lie between the H_3-type site and the R-type sites, as schematically shown in Fig. 1. For K, the stable adsorption sites are T_4-like which are very close to corresponding T_4-type sites. Starting from the H_3-type sites, the calculations would converge to the H_3-like sites in between the H_3-type and its nearby R-type sites, while the B_2-like sites converged from the B_2-type sites only deviate slightly from the starting configurations.

In Table I, we present the calculated binding energies along the line marked in Fig. 1. The binding energy is defined as

$$E_b = (E_{\text{surf}} + E_{\text{metal}}) - E_{(\text{surf+metal})},$$

where $E_{\text{metal+surf}}$ is the total energy for the semiconductor surface with a single metal atom adsorbed. The $E_{\text{metal}}+E_{\text{surf}}$

TABLE I. The binding energies for the sites as labeled in Fig. 1. The unit is eV.

	FHUC				UHUC			
Site	K	Cu	Ag	Au	K	Cu	Ag	Au
A	1.23	2.40	1.91	2.75	1.15	2.36	1.87	2.71
B_2^*	1.27	2.27	1.80	2.60	1.19	2.24	1.77	2.58
H_3	1.55	3.01	2.05	2.64	1.46	2.92	1.97	2.56
B_2	1.71	2.95	2.12	2.72	1.61	2.85	2.01	2.61
T_4	1.71	2.67	1.82	2.32	1.62	2.60	1.71	2.26
R	1.56	2.52	2.04	2.79	1.47	2.46	1.98	2.74
T_4'	1.75	2.69	1.82	2.33	1.69	2.64	1.75	2.31
B_2'	1.73	2.95	2.11	2.70	1.66	2.88	2.05	2.64
H_3'	1.54	2.98	2.02	2.60	1.51	2.94	1.99	2.59
$B_2^{*\prime}$	1.26	2.27	1.80	2.60	1.22	2.26	1.79	2.60
A′	1.23	2.40	1.91	2.75	1.19	2.38	1.90	2.74

was calculated by placing a metal atom above the semiconductor surface with its distances to Si atoms being >12 Å and to the terminating H atoms in the image of semiconductor surface being >11 Å. By our definition, the positive binding energy corresponds to an exothermic reaction, which means that the higher the binding energy the more stable the state. We see from Table I that the binding strength is stronger for Cu, Ag, and Au atoms than that for K atom. Starting from the optimized adsorption sites in Fig. 1, we fully relaxed the position of the adsorbate and the structure of the surface to obtain the low-lying adsorption sites for all these metal atoms The corresponding binding energies for the stable and the metastable sites for each hexagonal region adjacent to the corresponding Si adatom are tabulated in Table II, and the sites are marked as H_3-like and B_2-like sites for Cu, Ag, and Au as schematically shown in Fig. 1, and T_4-like and B_2-like sites for K which just deviate slightly from the corresponding T_4-type and B_2-type sites, respectively. A weak interaction between the metal atom and surface in the reference was removed by increasing the height of metal atom to above 12 Å compared to the 8 Å as used in our previous paper (Ref. 14). Also, recently, we found that the binding energies for the A-type, R-type, and B_2^*-type sites in our previous paper were underestimated by a computational inconsistency in fixing the silicon atoms both on the first and the second bottom layers while the data for the other sites were calculated using the structure with only the first bottom silicon atom layer fixed, the same as the reference surface. For the other sites, the current data as shown in Tables I and II are in agreement with the previous data. Though the fault in dealing with the A-type, R-type, and B_2^*-type sites does not affect the conclusions in the previous paper, the comparison in binding energy between the on-top dangling-bond sites and the other sites was affected, and the current data in this paper could act as a correction for these sites. The relative energies among the other sites are consistent.

The binding energies for K atom in H_3-like and B_2-like sites are about 20 meV lower compared to that of the corresponding T_4-like site in the corner and in the center hexagonal regions for both FHUC and UHUC, which are in good agreement with results from Cho and Kaxiras.[16] In each hexagonal region adjacent to the corresponding Si adatom of both half unit cells, the B_2-like and T_4-like sites for K atom have almost the same binding energies as those of the corresponding B_2-type and T_4-type sites, for they in fact deviate little in space, respectively. The K atom in H_3-like site moves a little toward the nearby R-type site compared to the H_3-type site, but the binding energy gains as much as about 140 meV. As listed in Table II, the B_2-like and the T_4-like

TABLE II. The binding energies in eV for the stable and metastable adsorption sites for the corner and center hexagonal regions in both half unit cells.

	FHUC				UHUC			
Site	K	Cu	Ag	Au	K	Cu	Ag	Au
H_3-like		3.02	2.22	2.90		2.93	2.13	2.82
B_2-like	1.71	3.07	2.20	2.87	1.61	2.98	2.11	2.79
T_4-like	1.71				1.63			
H_3'-like		2.98	2.18	2.83		2.94	2.13	2.79
B_2'-like	1.73	3.07	2.19	2.86	1.67	3.02	2.14	2.84
T_4'-like	1.75				1.69			

TABLE III. The difference in total energy between the best adsorption sites in both hexagonal regions adjacent to the corner and center Si adatoms for FHUC and UHUC. The numbers were calculated by subtracting the total energy of the stable state in the corner hexagonal region from that of the stable adsorption site in the center hexagonal region. The unit is meV. The experimental data were cited from Ref. 14.

	FHUC		UHUC	
Atom	Cal.	Expt.	Cal.	Expt.
Cu	−4	50	−31	−30
Ag	26	>80	−10	−5
Au	40	30	−25	−30

sites in the corner hexagonal region of FHUC have the same binding energies. However, for the convenience of discussion, we still would call T_4-like site the stable adsorption site. In the central hexagonal region of FHUC, the T_4'-like site has ~20 meV higher binding energy than that of the B_2'-like site. In UHUC, the highest binding-energy sites are T_4-like and T_4'-like sites in the corner and the center hexagonal regions, respectively.

Unlike the K atom, the Cu, Ag, and Au atoms have a significant higher binding energy in B_2-like sites than in the corresponding B_2-type sites. While the Cu atom likes to adsorb at the B_2-like sites in both corner and center hexagonal regions for both FHUC and UHUC, the Ag and Au atoms prefer the H_3-like site in the corner hexagonal region and the B_2-like site in the center hexagonal region for both half unit cells. In Table III, we compared the energy difference between the most stable sites in both hexagonal regions adjacent to the corner and to the center Si adatoms for Cu, Ag, and Au atoms with the experimental data.[14] The calculated data were computed by subtracting the total energy of stable adsorption site in the corner region from that of the stable adsorption site in the center region. Except for the Cu atom in FHUC, the data in Table III obtained with the spin-polarized calculations agree with the experimental results quite well and confirm the previous calculated results also.[14,37,42]

The average binding energies among the stable and metastable sites in FHUC and UHUC are around 1.70 and 1.68 eV for K, 3.04 and 2.97 eV for Cu, 2.17 and 2.16 eV for Ag, and 2.86 and 2.82 eV for Au, respectively. These data show that adsorption in the FHUC is preferred than that in the UHUC. The binding energies are K < Ag < Au < Cu for both half unit cells, showing the binding strength is Cu > Au > Ag > K.

B. Electronic properties

Since the triangle basin defined in Fig. 1 is representative for all the sites of interest in a half unit cell, and there is a great similarity between FHUC and UHUC owing to the similar chemical bonding, we would hereafter focus on discussing the electronic properties of the adsorption sites in the triangle basin in only one half unit cell.

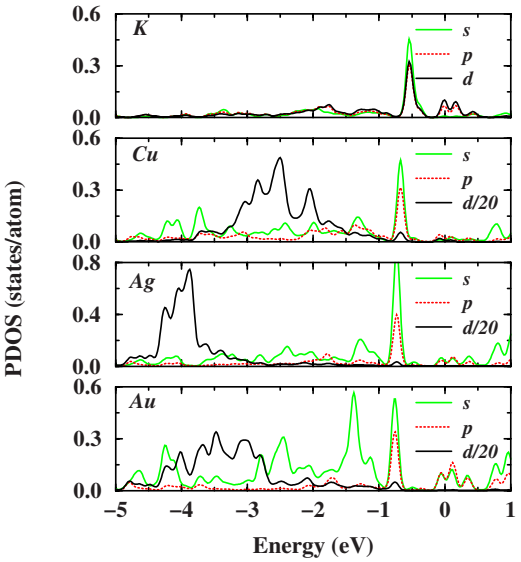

FIG. 2. (Color online) The partial density of states for Cu, Ag, and Au atoms adsorbed at the highest binding-energy adsorption sites and K at the B_2-like site for a direct comparison with the inside hexagonal region sites of Cu, Ag, and Au, in the basin of FHUC as defined by the triangle in Fig. 1. The gray (green) solid, black (red) dotted, and black solid lines are for the *s*, *p*, and *d* orbital, respectively. The *d* electron PDOS for Cu, Ag, and Au is reduced by a factor of 20.

By placing the metal atoms on the best adsorption sites in the corner and the center hexagonal regions, we have studied the electronic structures of the stable and metastable adsorption structures for each hexagonal region in both half unit cells. Figure 2 shows the studied partial density of states (PDOS) of adsorbates Cu, Ag, and Au atoms adsorbed on stable sites in the corner hexagonal region of FHUC, and K adsorbed on the B_2-like site for a direct comparison with those inside hexagonal region sites of Cu, Ag, and Au. We have projected the wave function on the *s*, *p*, and *d* orbitals for the adsorbed K, Cu, Ag, and Au atoms. K atom as shown in Fig. 2 has *s*, *p*, and *d* electron density in the shallow states below the *Fermi* energy, which should originate from the charge of the Si surface atoms. The *p* valence electrons of K atom itself are bound in the deep energy band with the band energy of about 15 eV below the *Fermi* energy, which is quite different from those of Cu, Ag, and Au and was not shown in Fig. 2. The *s* valence electron PDOS for Cu, Ag, and Au is widely broadened due to its strong interaction with the silicon surface. Due to the interaction with the surface, the metal atoms acquire some *p* character in the PDOS. In fact, the *s* and *p* PDOSs for Cu, Ag, and Au atoms shown in Fig. 2 have a similar overall curve profile compared to that of the Si surface. When there is strong interaction, the projection method cannot tell whether the charge density should "belong" to the metal atoms or the Si surface. Due to the large number of *d* electrons, the corresponding *d* orbital PDOS is the dominating component and the density shown in Fig. 2 is reduced by a factor of 20 in order to appropriately display the *s* and *p* curves for Cu, Ag, and Au atoms in the figure simultaneously. Besides the strong interaction of *s* valence electrons of the metal atoms with the surface, the inner

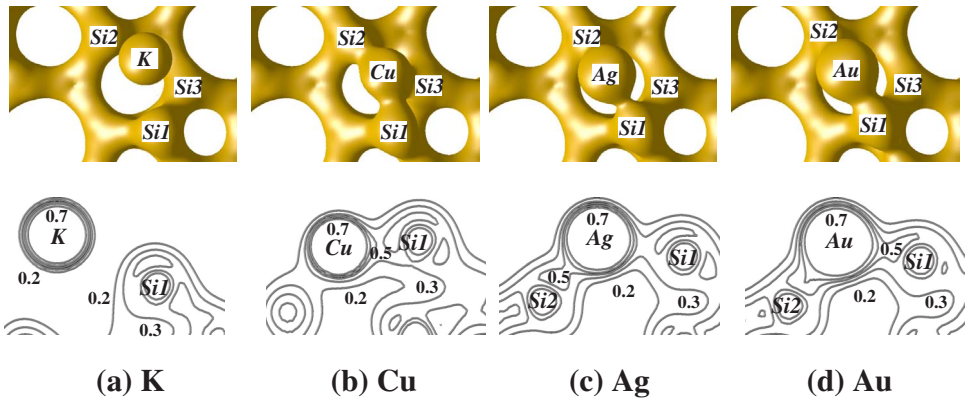

FIG. 3. (Color online) The charge density for Cu, Ag, and Au adsorbed on their highest binding-energy adsorption sites and K at the B_2-like site for a direct comparison with the inside hexagonal region sites of Cu, Ag, and Au, in the basin of FHUC as defined by the triangle in Fig. 1. (a), (b), (c), and (d) are for K, Cu, Ag, and Au atoms, respectively. For convenience of discussion, the nearby Si adatom and Si rest atom are marked as Si1 and Si2, respectively, and another nearby Si atom is marked as Si3. For each configuration, the upper figure is the isosurface of charge density at 0.3 $e/\text{Å}^3$ (top view), and the lower figure is the density contour in the plane perpendicular to the surface containing the corner Si adatom and the adsorbed metal atom. The unit in the lower figure is $e/\text{Å}^3$.

shell *d* electrons also have strong interaction with the surface judging from the broadening of the *d* levels in Fig. 2. The band energies of the *d* levels follow the order Cu > Au > Ag, implying interaction strength with the surface in the order of Cu > Au > Ag, in agreement with the calculated binding energies of these atoms as shown in Tables II and III.

The electronegativity of K is 0.82, much smaller than that of Si (1.90). It seems reasonable to think that the *s* electron of K is transferred to the surface. Its empty *s* orbital lies about 2.4 eV above the *Fermi* energy. The K atom would then like to develop ionic bond with the surface. On the other hand, the Cu, Ag, and Au have comparable electronegativities with Si, which are 1.90, 1.93, and 2.40, respectively. By the projection of the wave function on *s* orbital, we find that the PDOS of *s* electron is broadened greatly and basically has similar characteristic to the density of states (DOS) of the surface. This naturally introduces one question: what is the nature of the bonding between these atoms and the surface? To answer this question, we have studied the charge density of the best adsorption sites in corner and center hexagonal regions for both half unit cells. We have shown the results for the K, Cu, Ag, and Au atoms adsorbed in the corner hexagonal region of FHUC in Fig. 3. The upper panel gives the charge isosurface at 0.3 $e/\text{Å}^3$, while the lower panel shows the charge density contours in a plane that is perpendicular to the surface and contains the adsorbate and the corner Si adatom. In order to make the description clearly, we have marked in Fig. 3 the corner Si adatom as Si1, the Si rest atom as Si2, and the other nearby Si atom as Si3. There is a finite density of charge between the Cu, Ag, Au, and the nearby Si atoms (Si1 and Si2 for Ag and Au, while Si1, Si2, and Si3 for Cu). The charge density contours could further confirm the conclusion indicated by the isosurface. For the K atom, there is no charge density between K and Si atoms. By subtracting the charge density of adsorbed system from the separated charge density of K atom and the surface, keeping the corresponding coordinates unchanged from those of the adsorption system, we find that there is an obvious charge transfer from K atom to the surrounding Si atoms. However, this method does not give any indication about the charge transfer between Cu, Ag, Au, and the surface. In our previous studies,[14] we have also compared the charge densities of Ag at on-top Si adatom site, and the charge density of H atom at on-top Si adatom site. Although the charge density along the bond of adsorbate to Si atom is weaker for Ag than that for H, the value is comparable. Combined with the calculated charge density in Fig. 3, we would like to conclude that the bonding nature between Cu, Ag, Au, and Si atoms, with Cu, Ag, and Au atoms sit at the H_3-like or B_2-like sites, is covalent, although it is weaker than the well accepted covalent bond criterion for H adsorbed on Si(111)-(7×7) surface. Missing one electron, the cation K^+ sits in a multicoordinate site and form ionic bond with the nearby Si atoms.

The interatomic distances between the adsorbed metal atom and the nearby Si atoms for the best adsorption sites in the corner hexagonal region of the FHUC are listed in Table IV. For comparison, the interatomic distances for metal atom on atop of A- and R-type sites (see Fig. 1) are also included. The data for the corresponding sites in the center hexagonal region of the FHUC and in both the corner and center hexagonal regions of the UHUC are similar to those presented in Table IV. The distances of best adsorption sites from Si atoms are longer than those of A- and R-type sites, indicating the bonding becomes weaker for each single bond connecting the metal atom and the Si atom. The binding energies (see Table I) per bond for adsorbing on top of A- and R-type sites are around 2.46, 1.98, 2.77 eV for Cu, Ag, and Au, while they are on average only about 1.22, 0.88, and 1.15 eV for Cu, Ag, and Au at the best adsorption sites in corner hexagonal region of FHUC. Despite the decreasing strength per bond, the number of bonds increases for H_3-like and B_2-like sites. The competition between the bond strength and the number of bond results in that the H_3-like and B_2-like sites are more stable. For Au, we have noticed that most recently Ghose *et al.*[38] reported their experimental results measured by surface x-ray diffraction technique (SXRD). They detected the Au sitting at the multicoordinate bridge sites, which is in close agreement with our calculation results

TABLE IV. The interatomic distances between adsorbed metal atoms and its nearby Si atoms when they adsorb on stable, metastable, A, and R sites in the hexagonal region adjacent to the corner Si adatom in FHUC. The unit is Å.

Sites	Si1	Si2	Si3	Sites	Si1	Si2	Si3
K T_4-like	3.91	3.24	3.60	Ag H_3-like	2.59	2.48	3.22
B_2-like	3.30	3.28	3.62	B_2-like	2.57	2.51	2.83
A	3.18			A	2.39		
R	3.18			R	2.39		
Cu H_3-like	2.35	2.34	2.57	Au H_3-like	2.53	2.40	3.29
B_2-like	2.39	2.36	2.37	B_2-like	2.47	2.53	2.47
A	2.20			A	2.28		
R	2.20			R	2.29		

here. The favorable B_2-like and H_3-like sites are comparable in binding energy for Au adsorbed on Si(111)-7×7 surface, with a difference of only about 30 meV.

For the monovalent metal atoms involved in our study whose inner electronic shells are completed occupied with only one electron on the higher energy *s* orbital, the best adsorption sites are found to be different from that of the hydrogen atom. H atom is believed to sit on-top Si dangling bond forming a covalent bond. However, the K, Cu, Ag, and Au atoms actually like to sit on the multicoordinate sites. As discussed above, K is likely to lose its *s* electron to the surface to become a cation K^+ that favors multicoordinate sites by the electric attraction from the electron cloud surrounding the nearby Si atoms. Unlike the K atom and H atom, the *d* electrons in Cu, Ag, and Au could strongly affect the interaction with the surface and the bond length. With the interaction strength of *d* levels with the surface in the order Cu > Au > Ag, as shown in Table IV, the bond length between metal atom and Si atom generally also follows the order Cu < Au < Ag. Besides of the *d* electrons, the size of the atom is also a factor to determine the adsorption site. The covalent radii for Cu, Ag, Au, Si, and H are 1.32, 1.45, 1.36, 1.11, and 0.31 Å, respectively.[39] When Cu, Ag, and Au atoms sit on multicoordinate sites, they can form bonds with multiple nearby Si atoms with bond lengths around 2.5 Å, and thus increase the binding strength. However, the sum of covalent radii of Si and H is only 1.42 Å, which is too small to support multiple H-Si covalent bonds by sitting on B_2-like multicoordinate sites.

C. Simulated STM images

In the above description, we reach the conclusion that the studied metal atoms like to sit in multicoordinate sites instead of the sites on-top dangling bonds. However, the experiments show that the bright spots in STM images obtained under negative bias are located on-top Si adatoms for Cu, Ag, and Au atoms on Si(111)-(7×7) surface.[14] To understand the discrepancy between calculated best adsorption sites and the sites of bright spots in STM images, we have simulated the STM images using the Tersoff and Hamann approach.[40] We note that Custance *et al.*[41] reported their experimental and theoretical results of Pb adsorption sites. Pb was observed by STM at B_2-type site, identical with the simulated STM image position. Their results were well reproduced by our calculations.

Figure 4 shows the schematic position of the H_3-like and B_2-like sites for Cu, Ag, and Au adsorbed in the corner hexagonal region of FHUC. The H_3-like site for K is close to that of Cu, Ag, or Au, while its T_4-like and B_2-like sites are almost identical to the corresponding T_4-type and B_2-type sites, respectively. A T_4-type site is also marked out in the figure. By connecting the equivalent T_4-like, H_3-like, and B_2-like sites for K in the basin as defined by the triangle in Fig. 1 for the FHUC, we get a polygon as indicated in Fig. 4. We interpolated ten points between the T_4-like and B_2-like sites, and between B_2-like and H_3-like sites, respectively. By fully relaxing the surface, the energy barriers are estimated to be ~17 meV for the K atom diffusing from the B_2-like site to H_3-like site, and ~17 meV to the T_4-like site. This is to say that a K atom with an excess thermal energy of about 20 meV can diffuse around the R site along a path indicated by the polygon in Fig. 4. Even at low temperatures, the K should diffuse readily around the R site. We carefully

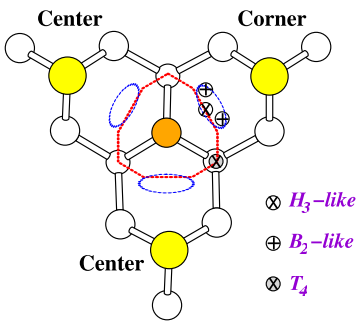

FIG. 4. (Color online) The schematic atomic configuration of the favorable adsorption sites: H_3-like, and B_2-like sites for the Cu, Ag, and Au atoms in the hexagonal region adjacent to the corner Si adatom of FHUC. For K, the H_3-like is close to the one marked in figure; the T_4-like and B_2-like are identical to T_4 and B_2 sites. A T_4 site is also marked out. The polygon connecting the equivalent H_3-like, B_2-like, and T_4-like type sites for K shows a probable diffusion path surrounding the Si rest atom. The ellipses roughly show the favorable diffusion areas of the Cu, Ag, and Au atoms at low temperatures.

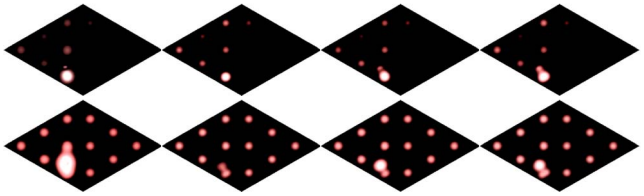

FIG. 5. (Color online) The simulated STM images for K, Cu, Ag, and Au atoms adsorbed in the hexagonal region adjacent to the corner Si adatom of FHUC. (a) is for the K atom adsorbed at B_2-like site, while (b), (c), and (d) are the superpositioned images for a single Cu, Ag, and Au atoms adsorbed at the H_3-like site and the two nearest-symmetrical B_2-like sites, respectively. For each configuration, the upper one is for −0.5 V bias while the lower one is for +2.0 V bias.

checked the possible diffusion paths in the triangle basin as marked in Fig. 1. While a K atom needs only ~20 meV to diffuse around the R site, it needs about 140 meV to escape from this basin to the neighboring equivalent basins. For the Cu, Ag, and Au atoms, the conditions are different. As shown in Fig. 4, the ellipses show the favorable adsorption areas. We interpolated ten points between the H_3-like and B_2-like sites for Cu, Ag, and Au on the potential surface. The optimized configurations by fully relaxing the surface show that a single Cu, Ag, and Au atoms needs about 50, 10, and 60 meV to diffuse from the stable adsorption site to the metastable adsorption site within the area roughly defined by the ellipse in Fig. 4. This indicates that the potential surface inside the ellipse is quite flat, showing that the Cu, Ag, and Au atoms could diffuse almost freely within this area at low temperatures. Careful analysis of the adsorption sites shows that a single Cu, Ag, and Au atom needs to overcome about 380, 180, and 160 meV to diffuse to the neighboring ellipse area, significantly larger than that for K.

In Fig. 5, we show the simulated STM images. The upper figures are the images at the −0.5 V bias, and the lower figures are the images at 2.0 V bias. Figure 5(a) shows the images for K adsorbed at the B_2-like site. Under negative bias, the corner silicon adatom site is bright while the K atom at B_2-like site is invisible. Under positive bias, a big bright area covering the Si adatom site and the B_2-like site appears. Due to the fast diffusion of the K atom surrounding the R site along the polygonal path indicated in Fig. 4, the whole basin defined by the triangle in Fig. 1 would be bright even at low temperatures. At an elevated temperature, the K would diffuse among the whole half unit cell, and the whole half unit cell would become bright uniformly. With a diffusion energy barrier of only about 20 meV for K along the polygonal path, it would be hard to trap a single K atom at a B_2-like position, and the images shown in Fig. 5(a) would not be observable experimentally. By placing a single Cu, Ag, and Au atoms at its best adsorption sites, our simulated STM images show the bright spots at the nearby Si adatoms under negative bias but bright spots at the adsorbed metal atoms at positive bias. As discussed above, the Cu, Ag, and Au atoms would diffuse fast within the area roughly defined by the ellipse in Fig. 4. So, the measured STM image must be a superposition of simulated images for the Cu, Ag, and Au atoms sitting at the H_3-like site, B_2-like and its symmetrical equivalent B_2-like sites (see Fig. 4), as shown in Figs. 5(b)–5(d), respectively. In the negative −0.5 V bias images, the Si adatom sites are bright while the metal atoms are almost invisible. In the positive 2.0 V bias images, all of the Si adatoms and the metal-atom sites are bright. These simulated images agree very well with the experimental images obtained at 77 K.[14]

TABLE V. The height of metal atoms and its nearby Si atoms when the metal atom adsorbs at stable and metastable sites in the hexagonal region adjacent to the corner Si adatom in FHUC. The number in brackets gives the height increase induced by the adsorption. The heights of the corresponding Si atoms for bare surface are also tabulated for comparison. The unit is Å and the plane containing the three Si rest atoms in FHUC of bare surface is chosen as the reference.

Sites	Metal	Si1	Si2	Si3
Bare Surface		0.90	0	−0.46
K T_4-like	2.36	0.98 (0.08)	−0.10	−0.46 (0.0)
B_2-like	2.64	1.14 (0.24)	−0.09	−0.39 (0.07)
Cu H_3-like	0.98	1.29 (0.39)	−0.22	−0.42 (0.04)
B_2-like	1.06	1.23 (0.33)	−0.19	−0.50 (−0.04)
Ag H_3-like	1.63	1.01 (0.11)	−0.23	−0.47 (−0.01)
B_2-like	1.56	1.17 (0.27)	−0.20	−0.41 (0.05)
Au H_3-like	1.61	1.03 (0.13)	−0.30	−0.48 (−0.02)
B_2-like	1.28	1.35 (0.45)	−0.17	−0.54 (−0.08)

Unlike Ag and Au, the image of Cu atom shown in Fig. 5(b) is dimmer as compared to the bright images for Ag and Au atoms. By carefully checking the coordinates, we attribute this to the different heights for the Cu, Ag, and Au atoms on the surface. We present the heights of the metal atoms and its nearby silicon atoms for a single metal atom adsorbed at stable and metastable sites in Table V. The labels of Si1, Si2, and Si3 are the same as those in Fig. 3. The adsorptions of Cu, Ag, and Au push up the nearby Si adatoms (Si1 atoms), which contribute to their higher brightness under negative bias. One can see that the Cu atom sits at about 1.02 Å above the reference plane, while the Ag and Au atoms are about 1.60 and 1.44 Å above the reference plane. The lower position of Cu compared to those of Ag and Au atoms is a reason for the different brightness in the simulated positive bias images. We also note the changes in heights of the nearby Si rest atoms (Si2 atom) and the other nearby Si atoms (Si3 atoms). The heights of Si2 atoms are reduced by about 0.2 Å for Cu, Ag, and Au adsorptions, while those of Si3 atoms show little changes. The bonding of Cu, Ag, and Au on the H_3-like and B_2-like sites saturates both the Si1 and Si2 dangling bonds, leading to a large change in the local charge that induce obvious changes in the height of these atoms. However, charge redistribution does not affect the heights of Si3 much. The K sitting at B_2-like site atom transfers its *s* electrons to the surface, and the induced charge redistribution leads to obvious changes in the height of Si1 atom. The K atom is found to be positioned at more than 1.5 Å higher than Si1 atom (much higher than

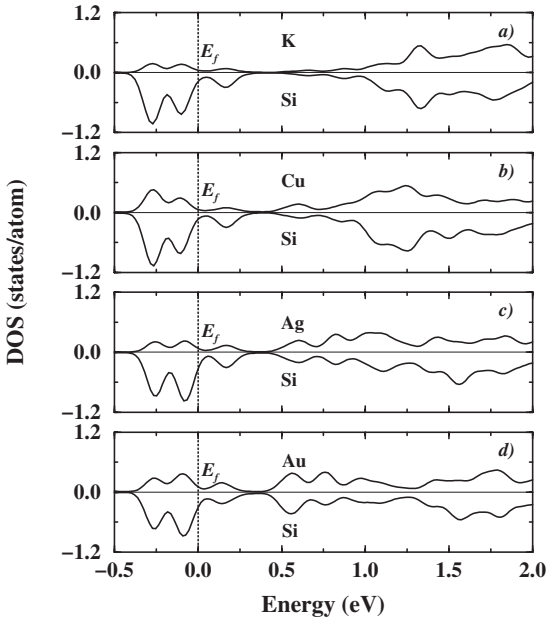

FIG. 6. The density of states of the single K, Cu, Ag, and Au atoms and their nearest Si adatoms when they adsorb at the B_2-like, B_2-like, H_3-like, H_3-like sites, respectively, in the hexagonal region adjacent to the corner Si adatom of FHUC. (a), (b), (c), and (d) are for K, Cu, Ag, and Au atoms, respectively. In each panel, the upward curve is for the metal atom while the downward curve is for the corner Si adatom.

Ag, Au, and Cu atoms, and >2.6 Å above the reference plane), which should be quite conspicuous in STM images. However, the K atom loses its *s* electron and the *p* level is pinned deep in energy, and as a consequence, the cation K^+ has no filled density of states in the neighborhood below the *Fermi* level. This is why it is not observed under negative bias in the simulated STM image in Fig. 5(a). Only the nearby Si adatom which gains much charge becomes a bright spot in the simulated STM image as shown in the upper panel of Fig. 5(a). Under positive bias, by tunneling into the density of states of unoccupied states above the *Fermi* level, we could see not only the Si adatoms but also the K^+ cation [lower figure of Fig. 5(a)].

Figure 6 shows the calculated density of states for the adsorbed metal atom and the corner Si adatom when K, Cu, Ag, and Au atoms are adsorbed at the B_2-like, B_2-like, H_3-like, and H_3-like sites, respectively, in the corner hexagonal region of FHUC. It clearly shows that the density of states in the energy range between −0.5 eV and the *Fermi* level are much more for the Si corner adatom than for adsorbed metal atom. However, the Si adatom has almost same density of states compared with the metal atom in the energy range from the *Fermi* level to 2.0 eV. These electronic structures characteristics are also consistent with the simulated STM images that at a negative bias the Si adatom are brighter and the metal atom are almost invisible; but at a positive bias the corner Si adatom and the corresponding metal atom have comparable brightness.

IV. CONCLUSIONS

We have theoretically studied the adsorptions of single Cu, Ag, Au, and K atoms on the highly reconstructed Si(111)-(7×7) surface. Cu, Ag, and Au atoms are found to sit on multicoordinate sites, and saturate the maximum number of dangling bonds. The *d* electrons as well as the *s* electron interact with the surface. The geometrical effect of the saturation of the dangling bonds is that the nearby Si adatom pops up, while it lowers the nearby Si rest atom. The height change combined with the charge redistribution induced by the adsorption of the foreign metal atom results in bright spot on the nearby Si adatom in the simulated STM images under a negative bias. However, under a positive bias not only the Si adatoms but also the K, Cu, Ag, and Au atoms could be seen. The adsorbed Cu, Ag, and Au atoms on multicoordinate sites form several weak bonds with the nearby Si atoms. The finite charge density between adsorbed Cu, Ag, or Au metal atom and Si indicates that these bonds are covalent in nature. K atom favors the T_4-like site while the H_3-like- and the B_2-like-type sites have almost the same binding energies. The charge transfer to the nearby Si adatom from the K atom makes the Si adatom brighter than the other Si adatoms in the simulated negative bias STM image. The nature of the bond between K and Si is ionic. Our results were consistent with experimental STM observations and represented a systematic study of adsorption of hydrogen-like atoms on Si(111)-(7×7).

ACKNOWLEDGMENTS

We thank the Center for Computational Materials Science of the Institute for Materials Research, Tohoku University for their continuous support of the SR11000 supercomputing facilities. X.D. acknowledges the financial support from the Research Grants Council of Hong Kong (Grant No. RGC 604504). C.T.C. acknowledges the support of HKUST through Grant No. RPC06/07.SC21. X.G.G. is partially supported by the research program of MOE and Shanghai municipality.

[1] K. Bromann, C. Félix, H. Brune, W. Harbich, R. Monot, J. Buttet, and K. Kern, Science **274**, 956 (1996).
[2] H. Brune, M. Giovannini, K. Bromann, and K. Kern, Nature (London) **394**, 451 (1998).
[3] S. Sun, C. B. Murray, D. Weller, L. Folks, and A. Moser, Science **287**, 1989 (2000).
[4] L. Vitali, M. G. Ramsey, and F. P. Netzer, Phys. Rev. Lett. **83**, 316 (1999).
[5] M. Y. Lai and Y. L. Wang, Phys. Rev. B **64**, 241404(R) (2001).
[6] J. L. Li, J. F. Jia, X. J. Liang, X. Liu, J. Z. Wang, Q. K. Xue, Z. Q. Li, J. S. Tse, Z. Zhang, and S. B. Zhang, Phys. Rev. Lett. **88**, 066101 (2002).
[7] St. Tosch and H. Neddermeyer, Phys. Rev. Lett. **61**, 349 (1988).
[8] H. Hirayama, H. Okamoto, and K. Takayanagi, Phys. Rev. B **60**,

14260 (1999).
[9] T. Jarolímek, J. Mysliveček, P. Sobotík, and I. Ošt'ádal, Surf. Sci. **482–485**, 386 (2001).
[10] P. Sobotík, P. Kocán, and I. Ošt'ádal, Surf. Sci. **537**, L442 (2003).
[11] I. Chizhov, G. Lee, and R. F. Willis, Appl. Phys. A: Mater. Sci. Process. **66**, S1003 (1998).
[12] W. Mönch, *Semiconductor Surfaces and Interfaces* (Springer, Berlin, 2001) (and references therein).
[13] C. J. Chen, *Introduction to Scanning Tunneling Microscopy* (Oxford University Press, New York, 1993).
[14] C. Zhang, G. Chen, K. Wang, H. Yang, T. Su, C. T. Chan, M. M. T. Loy, and X. Xiao, Phys. Rev. Lett. **94**, 176104 (2005).
[15] K. Cho and E. Kaxiras, Europhys. Lett. **39**, 287 (1997) and references therein.
[16] K. Cho and E. Kaxiras, Surf. Sci. **396**, L261 (1998).
[17] K. Wu, Y. Fujikawa, T. Nagao, Y. Hasegawa, K. S. Nakayama, Q. K. Xue, E. G. Wang, T. Briere, V. Kumar, Y. Kawazoe, S. B. Zhang, and T. Sakurai, Phys. Rev. Lett. **91**, 126101 (2003).
[18] K. Takayanagi, Y. Tanishiro, S. Takahasi, and M. M. Takahasi, Surf. Sci. **164**, 367 (1985).
[19] J. J. Boland, Adv. Phys. **42**, 129 (1993).
[20] R. L. Lo, I. S. Hwang, M. S. Ho, and T. T. Tsong, Phys. Rev. Lett. **80**, 5584 (1998).
[21] A. Vittadini and A. Selloni, Phys. Rev. Lett. **75**, 4756 (1995).
[22] K. D. Brommer, M. Galván, A. D. Pino, Jr., and J. D. Joannopoulos, Surf. Sci. **314**, 57 (1994).
[23] G. A. Reider, U. Höfer, and T. F. Heinz, J. Chem. Phys. **94**, 4080 (1991).
[24] M. C. Flowers, N. B. H. Jonathan, Y. Liu, and A. Morris, J. Chem. Phys. **102**, 1034 (1995).
[25] T. Klitsner and J. S. Nelson, Phys. Rev. Lett. **67**, 3800 (1991).
[26] *Handbook of Chemistry and Physics*, edited by D. R. Lide (CRC, New York, 2001).
[27] P. Hohenberg and W. Kohn, Phys. Rev. **136**, B864 (1964).
[28] W. Kohn and L. Sham, Phys. Rev. **140**, A1133 (1965).
[29] G. Kresse and J. Hafner, Phys. Rev. B **47**, 558 (1993).
[30] G. Kresse and J. Furthmüller, Phys. Rev. B **54**, 11169 (1996).
[31] G. Kresse and D. Joubert, Phys. Rev. B **59**, 1758 (1999).
[32] P. E. Blöchl, Phys. Rev. B **50**, 17953 (1994).
[33] J. P. Perdew, K. Burke, and M. Ernzerhof, Phys. Rev. Lett. **77**, 3865 (1996).
[34] J. J. Scherer, J. B. Paul, C. P. Collier, and R. J. Saykally, J. Chem. Phys. **103**, 113 (1995).
[35] J. J. Scherer, J. B. Paul, C. P. Collier, A. O'Keefe, and R. J. Saykally, J. Chem. Phys. **103**, 9187 (1995).
[36] F. Rabilloud and C. Sporea, J. Comput. Methods Sci. Eng. **7**, 273 (2007).
[37] A subtle mistake in the real-space projection scheme was removed. Versions before VASP.4.5.4 such as the one used in Ref. 14 incorrectly extrapolated the real-space projection operators beyond the cutoff up to $r_{\mathrm{rl}}/100\times 101$. This usually induces an error about 1 meV per atom while in some cases the error can be up to a few meV per atom; G. Kresse and J. Furthmüler, *The Guide of the Vienna ab-initio Simulation Package* (Austria, 2007), available for download at http://cms.mpi.univie.ac.at/vasp.
[38] S. K. Ghose, P. A. Bennett, and I. K. Robinson, Phys. Rev. B **71**, 073407 (2005).
[39] B. Cordero, V. Gómez, A. E. Platero-Prats, M. Revés, J. Echeverría, E. Cremades, F. Barragán, and S. Alvarez, Dalton Trans. 2008, 2832.
[40] J. Tersoff and D. R. Hamann, Phys. Rev. Lett. **50**, 1998 (1983).
[41] O. Custance, S. Brochard, I. Brihuega, E. Artacho, J. M. Soler, A. M. Baró, and J. M. Gómez-Rodríguez, Phys. Rev. B **67**, 235410 (2003).
[42] K. Wang, G. Chen, C. Zhang, M. M. T. Loy, and X. Xiao, Phys. Rev. Lett. **101**, 266107 (2008).